Study on crack branching control technology that contributes to the improvement of arrest property of steel plates
厚鋼板アレスト特性改善に寄与するき裂分岐制御技術の探索

研究代表者　東京大学大学院工学系研究科　准教授　川畑　友弥

1. Introduction

Currently, steel materials are widely used for transportation and energy storage as well as in large structures for buildings and civil engineering. In recent years, from the viewpoint of construction cost, the sizes of structures have remarkably increased, and the thickness and strength of the steel plates used have correspondingly increased. In general, the toughness of steel materials with the same microstructure decreases with increasing plate thickness, and the risk of brittle fracture increases [1]. It has been thought crack branch can enhance the crack arrest property. However, no actual technology in steel structural field was proposed so far.

Crack branches from brittle fracture are also seen in daily life. When a crack propagates through a material, crack branching and bending sometimes occur. For example, when the windshield of an automobile is destroyed, many branches appear along with the crack propagation; the number of branches is remarkably high as the branches are used for absorbing energy, so it is conceivable that the crack branching has propagation arresting effects. Does the amount of energy dissipated increase due to the microbranches of the crack, decreasing the driving force, or does the driving force of each crack tip decrease since the two cracks propagate in parallel? Is it a combination of these two ideas? The conclusion is not clear. As a first step, we hope to understand the mechanical factors that dominate the fracture surface irregularities and crack branches.

In the present study, to clarify the mechanism of the crack branching phenomenon during fast crack propagation, we observe the relationship between the roughness of the fracture surface and the driving force and, in particular, the cause of the branching phenomenon particular to steel is examined.

2. Brittle crack branching by large-scale wide plate testing and fracture surface roughness

To realize long-distance brittle crack propagation, where reaching a crack branching condition is possible, ESSO tests have been conducted under constant low temperature using a 10 MN large-scale test machine, as is shown in Fig. 1. For details,

please refer to our recent paper [2]. A normalized steel plate (N30; YS416MPa, TS541MPa, vTrs-10deg.C) for a welding structure has been used as a test specimen. In the tests, two types of test specimens have been prepared as is shown in Table 1. The first type of test specimen comprised entirely N30 (#5), and the other type of test specimen was a sandwich structure (#3) where the hard part consisted of high-Ni steel to increase the plastic constraint, and the N30 zone was only 10 mm. Both parts have been joined by EBW (Electron Beam Welding).

Fig. 1 Ten MN tension testing machine used for wide plate tests

Table 1 Test conditions

#	Homogenous /Soft welded joint	Part A	Part B		Experimental conditions, Gross stress/Temperature
			Material	Width [mm]	
#3	Soft welded joint	High-nickel steel	N30	20	300 MPa/-100°C
#5	Homogenous		N30		300 MPa/-100°C

Both test piece outlines are shown in Fig. 2. Tensile stress has been applied from both ends through pins. In the tests, after controlling the temperature at a constant -100 °C, such as the usual ESSO test, a uniform tensile stress of 300 MPa was applied, and then, a crack has been artificially generated with blows from an air gun. To minimize the impact of the blows, we have used an impact energy as small as possible.

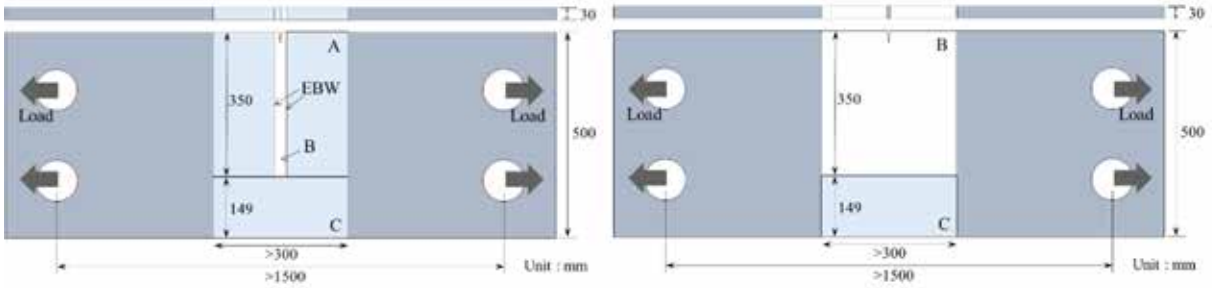

(a) #3 (b) #5

Fig. 2 Configuration of specimens

As a result of the tests, both specimens have shown clear branching of the brittle crack. Fig. 3 shows the fracture appearance and fracture surface observation results. Around the clear crack branching position, the fracture surface roughness changes drastically for both specimens. The first branching points occur at a crack length of 80 mm for # 3 and 160 mm for # 5.

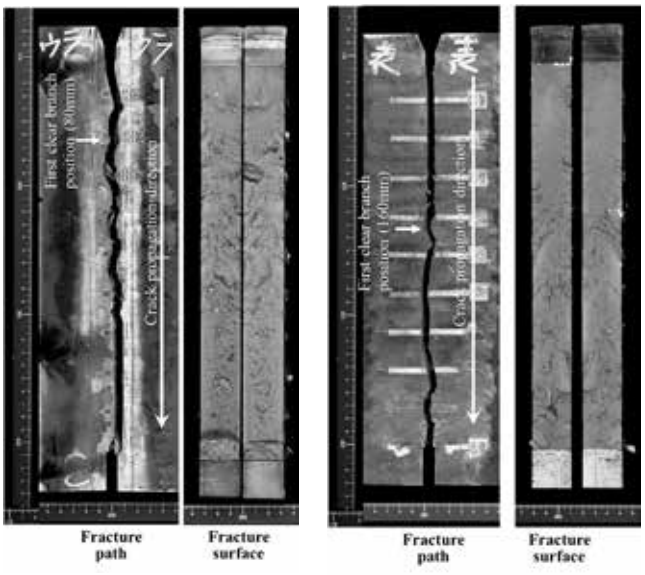

(a) Specimen #3 (b) Specimen #5

Fig. 3 Fracture appearance, fracture surface and crack branching position

Fig. 4 shows the crack propagation speed transition and the crack branching position. The propagation speed at the time of crack propagation is approximately 800 m/s, which is much lower than the theoretical value from the elastic fracture mechanics described in the previous section. As is confirmed by the visual observation of the roughness of the fractured surface, the surface is smooth up to the branching position, and the roughness dramatically increases in the vicinity of the crack branching.

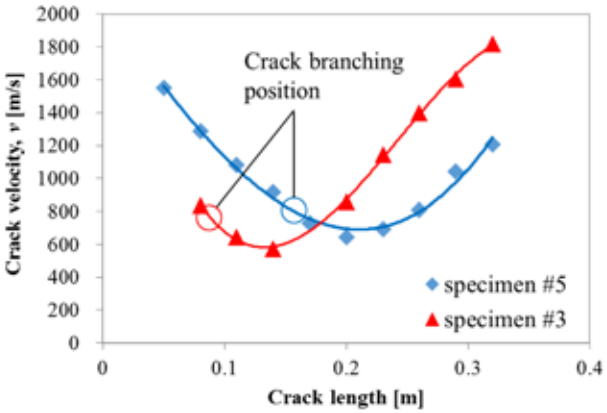

Fig. 4 Crack velocity and crack branching position

For an objective evaluation, the roughness is quantified. Fig. 5 shows the plots of the fracture surface roughness measured using a laser displacement metre (OPTEX-FA Co.; CD1-100N). The laser displacement metre irradiates a target area with laser light (the spot diameter of the focal area is 1 mm × 1.5 mm), and the distance to the target area can be precisely measured by the measurement of the time taken to receive the reflected light. The data measured are used as a roughness index by calculating the standard deviation in that region for each 5 mm width of the crack. The plots show that the fracture surface irregularities are conspicuous, after the crack

branch point is confirmed visually.

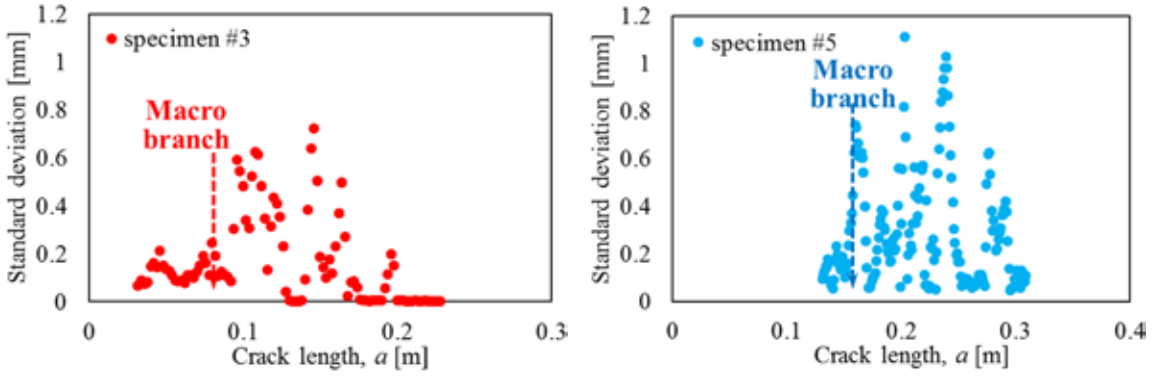

(a) (b)

Fig. 5 Surface roughness measurement results by laser displacement metre

To investigate the local critical conditions of the crack branches, FEM analysis is carried out. The model and sizes used are shown in Fig. 6. The finite element length in the crack propagation direction and longitudinal direction is set at 200 μm, which achieves both accuracy in the stress distribution evaluation and reasonable calculation costs. For the analysis, the stress-strain relationship obtained from the low-temperature high-speed tensile testing is used. To further realize actual mechanical conditions, the strength change in the heat affected zone from EBW welding is modelled. The increase of the strength in the heat affected zone is quantified by proportional calculations using the hardness tests. The crack tip shape is determined so that the stress intensity factor obtained from the stress values extracted from the elastically deformed region among the 20 elements in front of the crack tip is constant in the plate thickness direction.

(a) Overview

(b) Enlarged view of crack propagation area

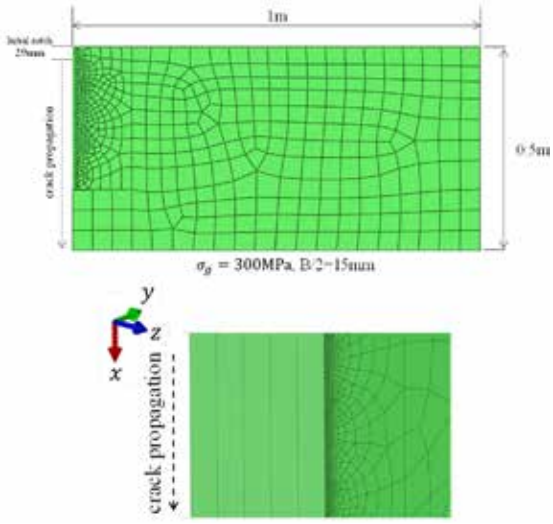

Fig. 6 Overview of FEM model for simulation

First, the validity of the circumferential stress criterion introduced by theoretical dynamic fracture mechanics [3] is examined for various crack length conditions. The circumferential stresses are calculated by the nodal stress data at the nearest (≒200～400 μm from the crack tip) nodes. However, the maximum circumferential stress is

observed at the zero-degree position like the static LEFM solution as is shown in Fig. 7. Only small increases in the circumferential stresses at non-zero degrees are observed compared with the LEFM solution. Thus, explaining the branching behaviour by the change of circumferential stress distributions is difficult.

In the present study, considering that crack branching perhaps occurs in markedly plastically deformed areas, the maximum principal stress at the crack tip and the stress triaxiality η are focused. The calculation results are shown in Fig. 8. Compared with the crack branching position in the experiment, the limit condition for crack branching is both σ_1>1500 MPa and t η>1.4. Again, these stresses must be focused so that branching does not occur in steel under the conditions of crack propagation speed shown from the theoretical solution by Yoffé [3]. We consider the micro mechanism corresponding to this focussing later. In addition, we confirmed the change in energy flux which is suggested by Nishioka et al. [4] does not develop into branching conditions.

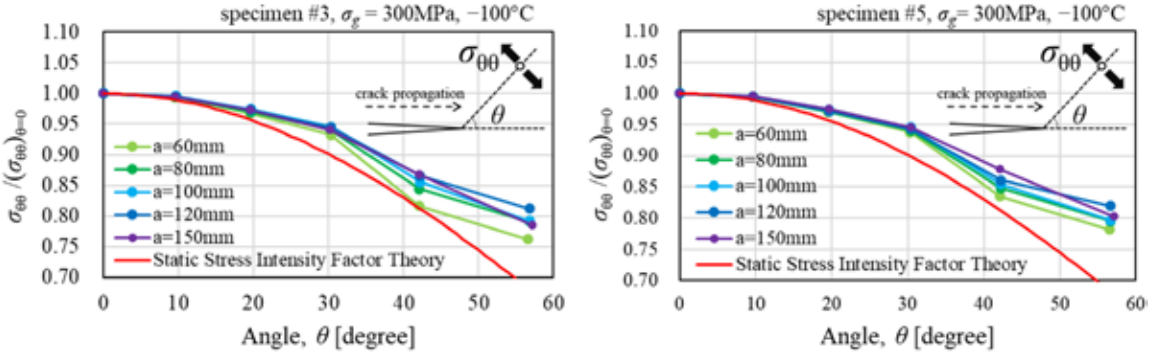

(a) Specimen #3　　(b) Specimen #5

Fig. 7　Calculation of circumferential stress variation

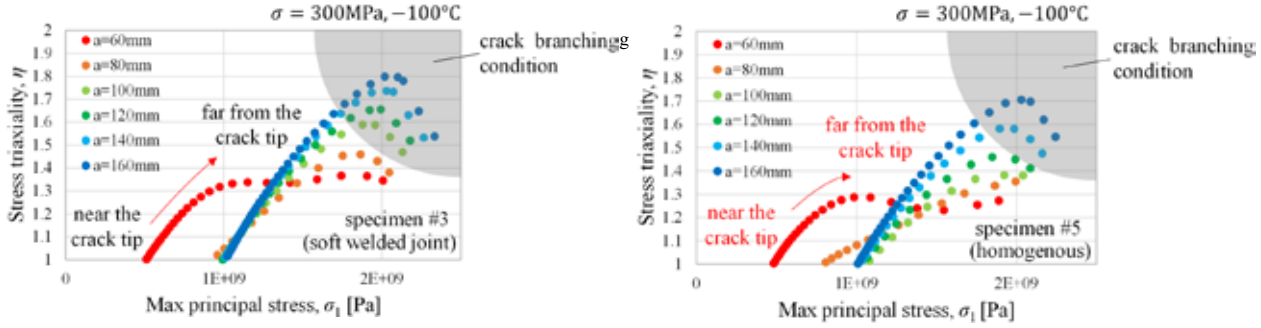

(c) Specimen #3　　(d) Specimen #5

Fig. 8　Increase of stress triaxiality and max principal stress under crack propagation

3. Small-scale brittle crack propagation test and fracture surface roughness

For the purpose of establishing a more accurate and simpler test method, we have developed a single edge-notched tension (SENT) test. A schematic of the test piece is shown in Fig. 9. The thickness of the evaluation area of the specimen is 10 mm. For this experiment, SM490A steel is used, which is the same kind of steel with same strength level as that used in Section 2. After uniform tensile stress is applied, brittle cracking is realized at an arbitrary time by the secondary loading.

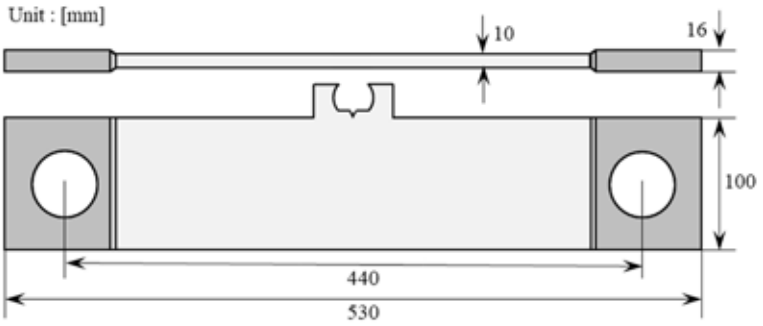

Fig. 9 Overview of SENT specimen

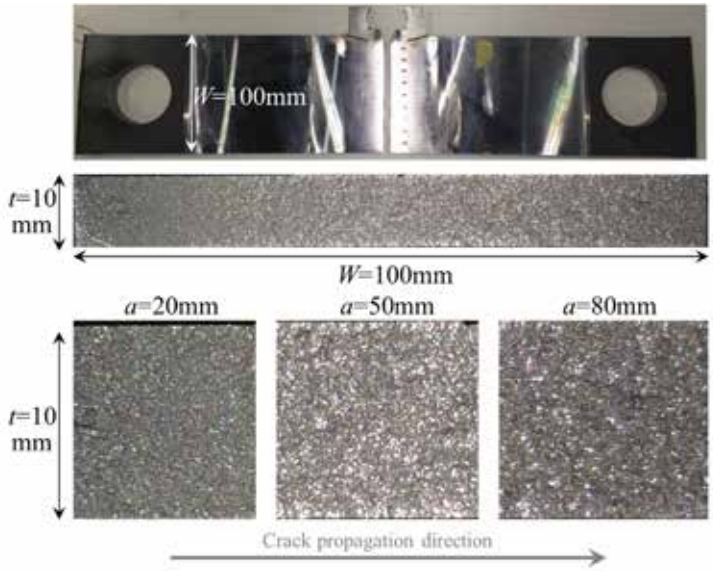

Fig. 10 Fracture appearance and fracture surface after SENT test

The test is carried out at temperature of -100 °C under load stress of 300 MPa. The temperature control is carried out in a spray-type cooling chamber, and the test is carried out after holding the temperature in the range of ±2 °C for 10 minutes or longer. The appearance and fracture surface of the specimen after the test are shown in Fig. 10. The cracks that have propagated are very straight, and no clear branching is observed in this test.

The fracture surfaces of this test tend to have less unevenness in the roughness than those of the ESSO test described in the previous section, and detailed analysis is difficult with the same laser displacement gauge. Therefore, we have obtained roughness data from stereo images taken with a scanning electron microscope (SEM). In this method, the height of the specimen surface is calculated from a pair of stereo

images acquired by SEM. The height information is obtained by photographing two inclined images and calculating the height by using the inclination angle. The principle of stereo photography is shown in Fig. 11.

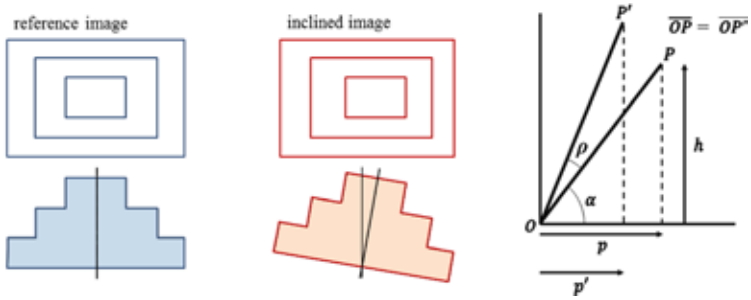

Fig. 11　General explanation of the principle of three-dimensional stereoscopic photography

A summary of the fracture surface roughness data obtained is shown in Fig. 12. The roughness becomes remarkable at crack length of 70 mm and then decreases. The crack propagation speed history shown in the lower part of Fig. 12 and the roughness are correlated. Additionally, at crack lengths greater than 70 mm, the roughness data obtained by the three-dimensional stereoscopic photography decreases, and so does the crack propagation speed. This decrease results from the stress relaxation due to the long crack propagation under the displacement control test.

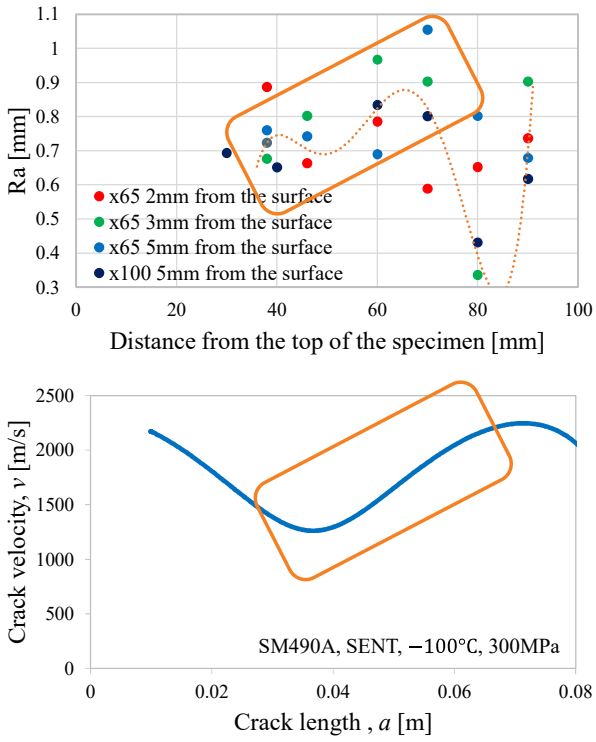

Fig. 12　Surface roughness acquired by SEM stereo photography and correlation with the crack velocity record

To obtain the detailed stress data around the running crack, FEM analysis is carried out with appropriate material constant input. The change in the crack tip stress field obtained by FEM analysis is shown in Fig. 13. Crack branching is not observed in this test piece, possibly because the crack branching condition suggested in the previous section is not satisfied. However, the stress field clearly rises as the crack progresses even if crack branching is not realized. As the main stress and the triaxiality increase, the roughness of the fracture surface first increases, and there may be a case where the stress finally reaches the branching condition at certain other conditions (e.g., a much lower temperature, thicker specimen, or side grooved specimen).

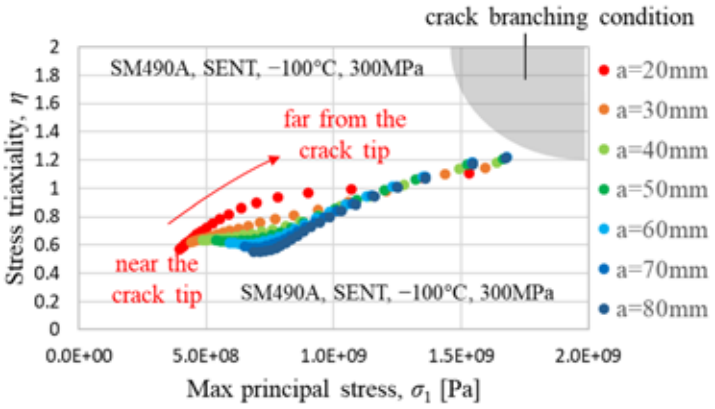

Fig. 13 Increase in the stress triaxiality and max principal stress under crack propagation (SENT, -100 °C) with the crack velocity record

Microcracks possibly occur at a position distant from the crack tip due to the expansion of the high stress region [5], where certain brittle phase particles may work as triggers for the initiation of microcracks, and cleavage facet planes with a large angle from the main fracture plane are chosen due to the rise in the stress triaxiality, as is schematically shown in Fig. 14. Thus, microcracks occur and propagate in the direction of this angle, which explains the increase in the roughness of the fracture surface. However, for macroscopic crack branches and stable growth, microcracks must

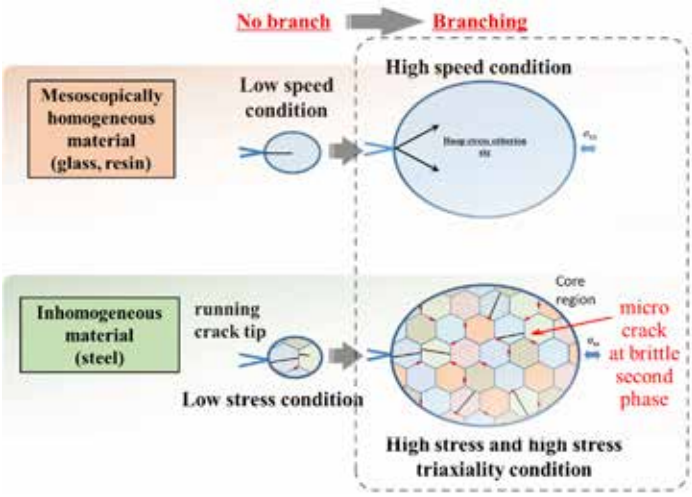

Fig. 14 Schematic explanation of the microscopic mechanism for the increase in the fracture surface roughness under high stress and stress triaxiality conditions

develop individually, for which criteria exist. Further detailed and quantitative examination is needed to understand the whole mechanism for crack branching behaviour in polycrystalline steel.

4. Conclusion

In this study, to clarify the mechanism of crack branching during brittle crack propagation, we have observed the relationship between the roughness of the fracture surface and the driving force and have discussed the cause of the particular branching phenomenon for steel.

The fracture surface roughness increases due to the crack propagation driving force, especially with increases in both the maximum principal stress and stress triaxiality, and branching is estimated to occur when both criteria are satisfied. This estimation has been validated by two different experiments using ordinary structural steel.

Microcracks in the high stress and high triaxiality region are more likely to be generated at different angles from the main fracture surface plane at positions separate from the crack tip. An increase in the crack propagation speed seems to correspond to an increase in the roughness in the SENT test. However, the increase in the propagation speed is not necessarily the direct cause for the increase in the fracture surface roughness but it is one of the results of the increase in the driving force, at least in steel. We think that the crack branching condition for steel, that is likely to occur at very low crack propagation speed, can be determined by local conditions, due to inhomogeneous microstructures.

ACKNOWLEDGEMENT

The authors of this work would like to express their gratitude to the JFE 21st Century Foundation. This work was supported by the Technical Research Aid of JFE 21st Century Foundation.

REFERENCES

[1] H. Kazuhiro, T. Nakagawa, S. Takeda, Y. Hashi, M. Tada, World's First Application of 47 kgf/mm^2 Higher Tensile Strength Steel for Large-Scale Container Ships and Realization of Safety Design to Respond to Trend for Supersizing, Mitsubishi Heavy Industries, Ltd., Technical Review Vol. 44 No. 3 (Sep. 2007)

[2] F. Tonsho, T. Kawabata, S. Aihara, Critical Condition of the Branching Behavior of Running Brittle Cracks in Steels, Modern Environmental Science and Engineering, February 2017, Volume 3, No. 2, pp. 136-142.

[3] E.H. Yoffé, On the moving Griffith crack, Philosophical Magazine, 42, 739,1951

[4] T. Nishioka, T. Kishimoto, Y. Ono, K. Sakakura, Basic Studies on the Governing Criterion for Dynamic Crack Branching Phenomena, Transactions of the Japan Society of Mechanical Engineers Series A, Volume 65 (1999) Issue 633 Pages 1123-1131.

[5] Y. Takashima, T. Kawabata, S. Yamada, F. Minami, Observation of Micro-Cracks Beneath Fracture Surface During Dynamic Crack Propagation, Theoretical and Applied Fracture Mechanics, Volume 92, December 2017, Pages 178-184.